RSC Advances

ROYAL SOCIETY OF CHEMISTRY

www.rsc.org/advances

Efficient synthesis of zirconium poly(styrene-phenylvinylphos-phonate)phosphate-supported proline as a recyclable catalyst for direct asymmetric aldol reactions in water

Chuanlong Wu[a*], Xiaoqing Long[a], Xiangkai Fu[b], Guangwei Wang[c*], Zakaria. A. Mirza[c]

[a]*Chongqing Unis Chemical Co, Ltd, National Enterprise Technology Center, Chongqing, 402161, PR China*
[b]*College of Chemistry and Chemical Engineering Southwest University, Chongqing, 400715, PR China*
[c]*Chongqing Institute of Green and Intelligent Technology (CIGIT), Chinese Academy of Sciences, Chongqing, 400714, PR China*
Tel: +86 2368253704; fax: +86 2368254000
E-mail: wcl110@swu.edu.cn

Abstract

A completely non-chromatographic and highly large-scale adaptable synthesis of zirconium poly(styrene-phenylvinylphos-phonate)phosphate-supported *L*-proline (**ZrPS-PVPA-Pr**) has been developed with only three steps overall. Catalyst **1c** was determined to be efficient for the asymmetric direct aldol reaction (only 0.5 mol% of **1c** was used) in the presence of water at room temperature, with an enantiomeric excess as high as 99%. In addition, water was identified to be one of the most significant reaction condition parameters due to the characteristics of the organic-inorganic hybrid catalyst support. Catalyst **1c** was easily recovered by simple filtration and could be reused at least six times with little loss of activity and enantioselectivity. Catalyst **1c** can be used efficiently on a large-scale while maintaining the enantioselectivities of the aldol reactions. Therefore, this method has the potential for application in industry.

Keywords: **ZrPS-PVPA-Pr**; Organic–inorganic hybrids; Heterogeneous catalysis; Aldol reactions; Large-scale; Green chemistry.

Introduction

The increasing quantities of industrial waste exert a significant and serious impact on the environment and force the modern chemical industry toward using clean processes due to the increasing demand of chemicals in various applications.[1-3] Therefore, to resolve this difficulty, the development and application of new types of heterogeneous catalysts for organic reactions is an important approach.

Industrially, condensation reactions are of great importance in the production of a number of key compounds. The direct asymmetric aldol reaction is one of the most important carbon-carbon bond-forming reactions and has been widely used in constructing natural and non-natural products.[4,5] Since the early reports in the 1970s on the *L*-proline catalysed intramolecular aldol reactions[6,7] and the discovery by List et al. that *L*-proline can mimic type Ⅰ aldolase to enantioselectively catalyse intermolecular aldol reactions,[8] interest in organocatalysis has significantly increased in the past few years due to the novelty of the concept and unique activation modes.[9-19] Many homogeneous chiral organocatalysts have been prepared, and many of these catalysts are known to be highly effective in asymmetric aldol reactions.[20,21] However, few examples of these catalysts have been developed for use in industrial processes, which is due to the un-avoidable drawbacks of homogeneous catalytic processes (e.g., short lifetime, lower structural and thermal stability, and difficulties in separation and recovery of highly expensive chiral catalysts), as well as concerns regarding product purity. Therefore, recycling and reuse of these expensive catalyst systems become important aspects. In addition, the separation of catalysts from product streams poses economic and environmental challenges.[22,23] Product separation, catalyst recovery, and resistance to drastic operational conditions, large-scale reactions are advantageous features of heterogeneous catalysts. A combination of these features would be desirable for establishing an ideal catalytic system.[24]

Currently, the immobilization of a chiral organocatalyst has been widely investigated on inorganic or organic supports, including mesoporous materials,[25] metals,[26] layered compounds,[27] polymers [28] and dendrimers.[29] However, the development of practical solid support-immobilized asymmetric catalysts has proven highly challenging due to lower enantioselectivities or efficiencies and number of use cycles. Therefore, new types of heterogeneous catalyst systems need to be developed.

In recent years, the zirconium phosphates and zirconium phosphonate field has been actively investigated, and the focus has primarily been on adsorbents,[30] inorganic ion exchangers,[31] intercalation chemistry,[32] catalyst supports and catalysts.[33,34] The stable amorphous L-proline-functionalized zirconium methyl-and/or phenylphosphonates were prepared to catalyse the direct asymmetric aldol addition with high yield, diastereoselectivity and enantiomeric excess.[35,36] The zirconium phosphate-phosphonate hybrid materials also have been extensively explored due to the large surface area, high thermal stability, good acid and chemical resistance, and advantage of that all of the organic groups were located on the surface of layers, interlamellar region and interlayer surface despite crystalline, semi-crystalline or amorphous nature of the solid. [37]

According to the theory and technique of hybridization or composition material, a hybrid or composite material exhibits new properties along with the original characteristics of each component. For the purpose of trying to synthesize a new type of organic-inorganic hybrid catalyst support that possesses quite different properties from either common organic support such as polystyrene or pure inorganic supports as silica gel, alumina, molecule sieve and zirconium phosphates or phosphonates, the frameworks of organic–inorganic hybrids **ZrPS-PVPA-Pr** were easily prepared in three steps overall. In addition, the method where the chiral organocatalyst is anchored onto **ZrPS-PVPA** (organic-inorganic hybrid support) has been rarely reported.

In line with the “green chemistry”, effective and environmentally benign synthetic methodology is often regarded as a goal in modern organic chemistry. The use of water, which has some advantages (i.e., cost, safety, and environmental impact), as a reaction solvent rather than an organic solvent is preferred to decrease environmental contamination in addition to the use of a catalyst support.[38-40] In addition, the surface of the supports as well as the caves, holes, pores, micropores and, channels in the supports may provide microenvironmental effects that exhibit different catalytic performances for asymmetric aldol reactions compared to those using either pure polystyrene or inorganic supports. In this paper, we report a new type of heterogeneous aldol reaction catalyst system using **ZrPS-PVPA** as a support, and this reaction proceeded efficiently in the presence of water at room temperature.

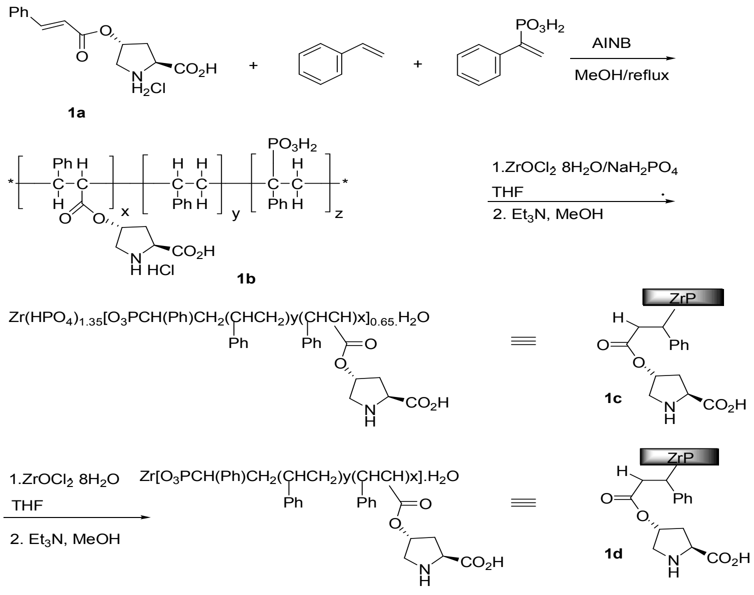

Scheme 1. Synthesis of catalysts **1c** and **1d**.

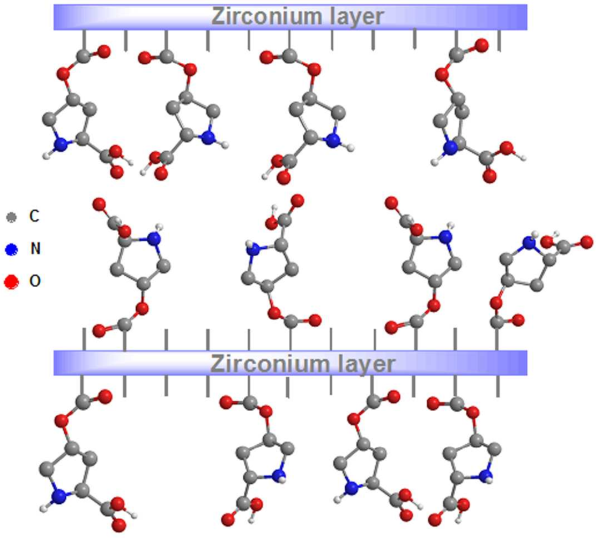

Figure 1. Ideal structural model of **ZrPS-PVPA-Pr**

Experimental

Materials and instrumentation

Hydroxyproline, styrene, styrene phosphoric acid and, cinnamic acid, were supplied by Alfa Aesar. All of the chemicals were used as received unless otherwise noted. The reagent grade solvents were distilled prior to use. The reactions were monitored by thin-layer chromatography (TLC) carried out on 0.25 mm silica gel plates, which were visualized using UV light and/or by staining with ethanolic phosphomolybdic acid (PMA) and/or ninhydrin in an ethanol stain.

Flash column chromatography was performed on silica gel (200-300 mesh). FT-IR spectra were recorded using KBr pellets on a Bruker RFS100/S spectrophotometer (USA) in the range of 400 0-400 cm^{-1}. The NMR spectra were recorded on a 300 MHz instrument. Chemical shifts (δ) are provided in ppm relative to TMS as the internal reference, and coupling constants (J) are reported in Hz. TG analysis was performed on a SBTQ600 Thermal Analyzer (USA) with a heating rate of 20 ℃·min^{-1} from 25 to 1000 ℃ under flowing N$_2$ (100 mL·min^{-1}). SEM was performed on a KYKY-EM3 200 (KYKY, China) microscope, with a resolution of 6.0 nm (30 kV) and a magnification range of 15X-250 000X. TEM images were obtained on a TECNAI10 (PHILIPS, Holland) apparatus, with a line resolution of 0.144 nm, and a point resolution of 0.282 nm, and magnification range of 25X-700 000X. The BET surface areas were determined using N$_2$ sorption data measured at 77 K (Quantachrome Autosorb-1). The sample was degassed at 100 □ for 8 h prior to obtaining the measurements. The pore size distribution curves were obtained from a desorption isotherm using the BJH method. Melting points were measured on a digital melting-point apparatus. Mass spectra (MS) were measured on HCT Bruker ESQUIRE LC/MS spectrometer with electrospray ionization. The elemental nitrogen content of the catalyst was determined using a Vario EL element analyser (Germany), with an Ar carrier gas. Analytical high performance liquid chromatography (HPLC) was carried out on an Agilent 1200 instrument using Chiralpak AD (4.6 mm×250 mm) or Chiralcel OD-H (4.6 mm×250 mm) columns. Optical rotations were measured on a JASCO P-1010 Polarimeter at λ=589 nm.

Catalyst synthesis

Synthesis of 1a [41-46]

A 1000 ml round bottom flask was charged with CF$_3$CO$_2$H (240 mL) and placed in an ice/water bath. Powdered *trans*-4-hydroxy-*L*-proline (500 mmol) was added in small portions under vigorous stirring to yield a viscous solution. The reaction mixture was stirred for 40 min, and then *trans*-3-phenylacryloyl chloride (750 mmol) was added in one portion. After 60 min of stirring, the mixture removed from the ice/water bath. The reaction flask was fitted with a loose glass stopper, and the reaction mixture was stirred at room temperature without any external temperature adjustment for 6 h, which yielded a clear and colourless solution. Then, the reaction flask was cooled in an ice/water bath, and Et_2O (500 mL) was slowly at first added under vigorous stirring over a period of 20 min. The resulting white suspension was stirred at 0-5 °C for 30 min after the addition was completed, followed by filtering by vacuum. The crystals were washed with two portions of Et_2O and dried at room temperature for 23 h in a ventilated hood to afford direct *O*-trans-3-phenylacryloyl proline hydrochloride **1a** (142.9 g, yield 96%).

Synthesis of 1b (PS-PVPA-Pr)

O-trans-3-phenylacryloyl proline hydrochloride **1a** (25.9 g, 86.8 mmol), 1-phenylvinyl phosphonic acid (8 g, 43.4 mmol), styrene (40 mL, 347.8 mmol), ethyl acetate (300 mL) and benzoyl peroxide (BPO, 5.0 g, 23.5 mmol) were used for the preparation of the PS-PVPA-Pr copolymer according to a previously published protocol.[47] Yield 36.75 g.

Synthesis of organic–inorganic hybrid zirconium phosphate catalyst 1c (ZrPS-PVPA-Pr)

PS-PVPA-Pr (10.0 g, 5 mmol), hydrated sodium orthophosphate (3.13 g, 20 mmol), $ZrOCl.8H_2O$ (8.05 g, 25 mmol) were used for the synthesis of organic-inorganic hybrid ZrPS-PVPA according to a previously published procedure.[47] Then, the pH of the reaction mixture was adjusted to neutral by addition of triethylamine followed by washing with distilled water and ethanol and subsequent drying under vacuum. The organic-inorganic hybrid solid ZrPS-PVPA-Pr was obtained in 91% yield. IR (KBr): v max/cm^{-1} 3405 (N-H); 3082, 2924 (CH); 3028 (-COOH); 1686, 1493, 756 ($-C_6H_5$); 1244, 1025 (P=O). (The mass fractions of the C, H and N, elements were determined by elemental analysis to be 39.88 mmol g^{-1}, 47.50 mmol g^{-1} and 0.125 mmol g^{-1}, respectively.)

Synthesis of pure organic zirconium phosphate catalyst 1d

PS-PVPA-Pr (10.0 g, 5 mmol) and, $ZrOCl.8H_2O$ (1.77 g, 5.5 mmol) were used for the synthesis of pure organic zirconium phosphate ZrPS-PVPA according to a previously published protocol.[47] Then, the pH of the reaction mixture was adjusted to neutral by addition of triethylamine followed by washing with distilled water and ethanol and subsequent drying under vacuum. The pure organic zirconium phosphate solid **1d** was obtained in 85% yield. IR (KBr): v max/cm^{-1} 3405 (N-H); 3059, 2923 (CH); 3025 (-COOH); 1686, 1453, 698 (-C_6H_5); 1247, 1029, 1025, and 999 (P=O). (The mass fractions of the C, H and N, elements were determined by elemental analysis to be 55.20 mmol g^{-1}, 61.09 mmol g^{-1}, and 0.182 mmol g^{-1}, respectively.)

General procedure for the direct aldol reaction using catalyst 1c in the presence of water

To a mixture of catalyst **1c** (10 mg, 0.125 mmol g^{-1} hydroxy-*L*-proline, determined according to N content of elemental analysis), cyclohexanone (1 mmol) and water (1 mL) were, stirred for 10 min at room temperature, and then aldehyde (0.25 mmol) was added. The reaction was monitored by TLC, and the mixture was filtered under vacuum and dried over anhydrous $MgSO_4$. Diastereoselectivity was determined by ^{1}H NMR or HPLC analysis of the crude aldol products. The enantiomeric excess (*ee*) was determined by chiral-phase HPLC analysis of the pure *anti*-product which was purified by flash column chromatography (Petroleum ether : EtOAC = 2:1). The absolute configuration of the aldol products was extrapolated by comparison of the HPLC-data with known literature data.

Results and discussion

Characterisation of the catalyst

FT-IR spectra analysis

To investigate the immobilization of hydroxyproline on ZrPS-PVPA, FT-IR spectra of catalysts **1c/1d** in the solid form were obtained, and the main absorption data recorded in the transmittance mode are shown in **Table 1**. The characteristic vibration bands at approximately 3405 cm^{-1} are due to the stretching vibration mode of N-H. In addition to other peaks located at 3059 cm^{-1}, 3082 cm^{-1}, 2923 cm^{-1}, 2924 cm^{-1} (CH); 3025 cm^{-1}, 3028 cm^{-1} (-COOH); 1686 cm^{-1}, 1493 cm^{-1}, 1453 cm^{-1}, 756 cm^{-1}, 698 cm^{-1} (-C_6H_5), these peaks demonstrated the successful anchoring of hydroxylproline onto the two different supports. According to the IR spectra of **1d**, the absorption peaks ranging from 999 cm^{-1} to 1247 cm^{-1} were assigned to the characteristic vibration of pure organic phosphonate. However, only two broad absorption peaks were observed at 1244 cm^{-1} and 1025 cm^{-1} in the IR spectra of **1c** due to the displacement, overlap and disappearance of peaks caused by the layered hybrid structure. The stretching vibration bands at 1244 cm^{-1} and 1025 cm^{-1} corresponded to the organic phosphonate and inorganic phosphate, respectively. These observations further confirmed the successful immobilization of hydroxylproline on the organic phosphonate and inorganic phosphate hybrid support (ZrPS-PVPA).

Table 1. IR absorption data of **1c** and **1d**.

Sample	IR, ν/cm^{-1}										
1c	3405	3082	3028	2924	1686	1493	1244	1025	756		
1d	3405	3059	3025	2923	1686	1453	1247	1029	1025	999	698

Surface morphology and micro-structure

The images obtained from scanning electron microscopy (SEM) and transmission electron microscopy (TEM) of catalysts **1c** and **1d** are shown in **Figure 2**, and these images indicated that heterogeneous catalyst **1c** was composed of amorphous particles with diameters of one hundred to several hundred nanometers. Each particle exhibits a loose structure due to the integration of various caves, holes, pores and channels with different shapes, structures and sizes (**Figure 2**, **A**). The TEM images show many micropores and secondary channels with diameters of approximately 25 nm among the layers of the catalyst after treatment in the presence of water. These micropores and secondary channels will increase the surface area of the catalysts and provide sufficient space for substrates to access the catalytic active sites (**Figure 2**, **C)**. However, in contrast to **1c**, catalyst **1d** exhibited aggregates with relatively fewer porous channels, due to the disorderly accumulation of amorphous particles with different diameters (**Figures 2**, B/D**)**. In general, one of the advantages of the layered zirconium phosphonate is that all of the organic groups were located on the surfaces, interlamellar regions and interlayer surfaces despite the crystalline, semi-crystalline or amorphous nature of the solid, which was determined by their self-assembled layered structure on the nanometer scale.

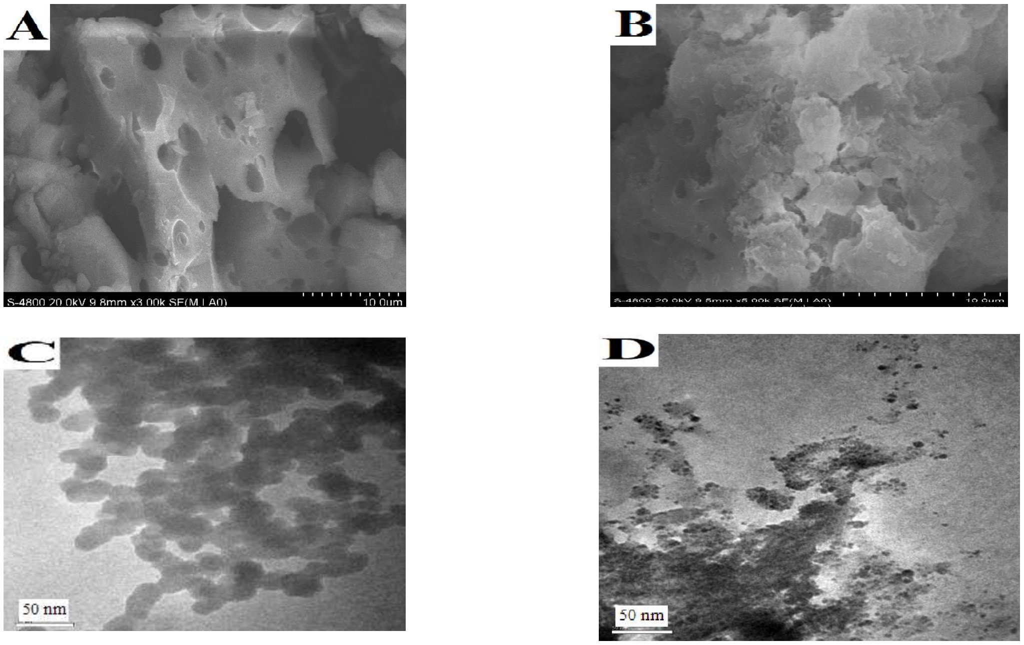

Figure 2. SEM (A: **1c**; B: **1d**) and TEM (C: **1c**; D: **1d**) analysis of catalysts **1c** and **1d**.

Using the X-ray diffractogram measurements of compounds **1c** and **1d** (**Figure 3**), the layer spacing was calculated. **1c** exhibited a larger layer spacing of 30.026 nm compared to pure organic zirconium phosphate **1d** (22.071 nm), which is due to changes in the electronic structure of the catalyst supports by addition of inorganic zirconium phosphate. The results indicated that the catalyst and substrate interact sufficiently in the adequate microenvironment among the layers of the heterogeneous catalyst bulk, as shown in the SEM and TEM images in **Figure 2**.

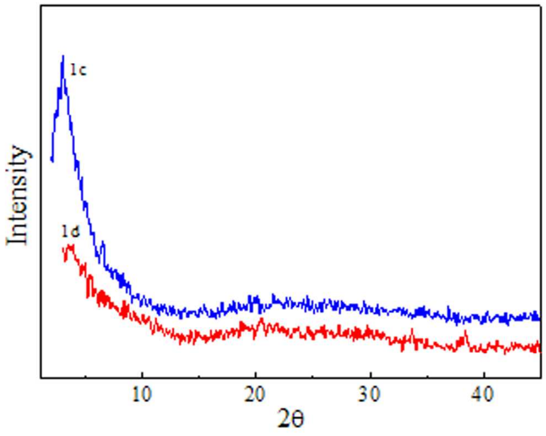

Figure 3. XRD pattern of catalysts **1c** and **1d**.

Elemental and BET surface area analysis

To determine the quantity of hydroxyproline immobilized on ZrPS-PVPA, we conducted elemental analysis of catalysts **1c** and **1d.** The mass fractions of C, H, and N were determined two times and are shown in **Table 2**. The relatively lower mass fraction of the N element in **1c** was due to the augmented molecular weight resulting from the addition of inorganic zirconium phosphate. Using the N_2 adsorption-desorption analysis (**Figure 4**), the BET surface and pore distribution of two types of polymeric immobilized catalysts were determined (**Table 2**). The results indicated that the organic-inorganic hybrid zirconium phosphate exhibited a significantly larger ratio surface area and pore volume than the pure organic zirconium phosphate. The results further confirmed the porous micro-structure in the heterogeneous catalyst bulk, as shown in **Figure 2**.

Table 2. Elemental analysis and N_2 adsorption-desorption analysis.

Catalyst	Times	C (%)	H (%)	N (%)	Surface area (cm^2g^{-1})	Pore volume ($\times 10^{-3}$ cm^3g^{-1})	Average pore diameter (nm)
1c	1	47.80	4.685	0.176	23.08	9.719	8.422
	2	47.91	4.824	0.174			
1d	1	66.28	6.032	0.25	4.50	2.096	9.313
	2	66.20	6.185	0.26			

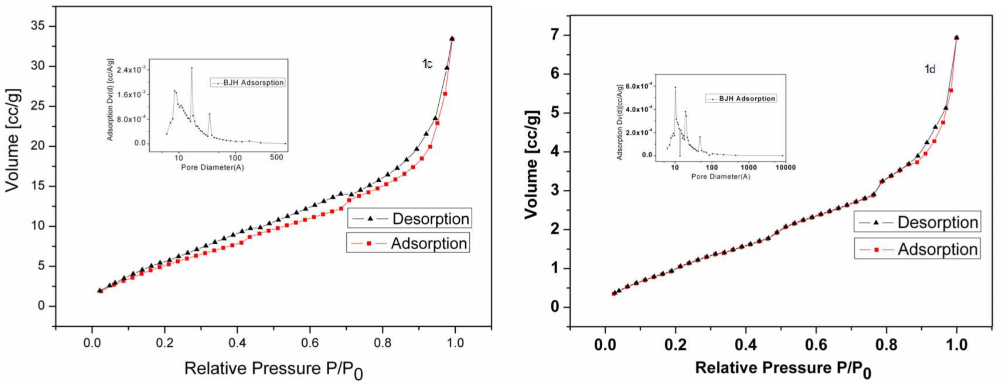

Figure 4. N_2 adsorption-desorption analysis of catalysts **1c** and **1d.**

Thermal stability

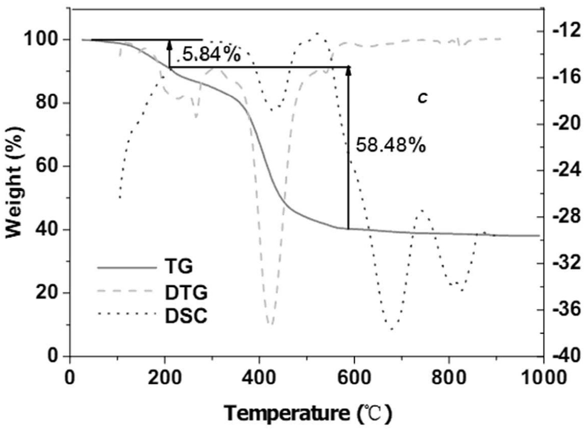

Figure 5. TG curves of catalyst **1c**.

To investigate the appropriate operational temperature range, the thermal analysis of catalyst **1c** was carried out, and the results are shown in **Figure 5**. The initial 5.84% weight loss observed from 20 to 200 °C was due to the crystallized water that was weakly bound to the material, and this result demonstrated the stability of catalyst **1c** up to approximately 200 °C. In the temperature range of 200-560 °C, two overlapping weight losses occurred due to the oxidation of organic portions of the catalyst. Above 560 °C, the weight losses were due to the dehydrolysis of $Zr(HPO_4)_2$ to ZrP_2O_7, and only cubic ZrP_2O_7 was observed at the end of the measurements at 1000 °C.

Asymmetry direct aldol reaction in the presence of water.

The heterogeneous catalytic performance was tested in the asymmetric direct aldol reaction using the typical reaction of cyclohexanone and *p*-nitrobenzaldehyde as a model for the chemical activity. All of the results are reported in **Table 3**. The performance of catalysts **1c** and **1d** strongly depended on the solvent in which the reaction occurred. To optimize the reaction conditions for the catalyst system, different solvents were investigated. When an organic solvent was used, the results were very poor. However, to our delight, the catalytic system proceeded efficiently in the presence of water (**Table 3**, entry 6).

Table 3. Solvent screening for the reaction between cyclohexanone and *p*-nitrobenzaldehyde.[a]

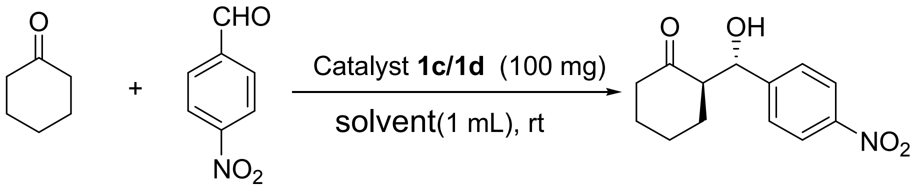

Entry	Catalyst	Cat. loading[mg]	Solvents	Yield[b] (%)	*anti:syn*[c]	ee[d] (%)
1	1c	100	-	60	53:47	44
2	1c	100	THF	55	54:46	42
3	1c	100	$CHCl_3$	53	63:37	36
4	1c	100	DMSO	65	68:32	43
5	1c	100	n-C_6H_{14}	45	76:24	65
6	**1c**	**100**	**water**	**99**	**85:15**	**93**
7	1d	100	-	58	56:44	14
8	1d	100	THF	55	54:46	37
9	1d	100	$CHCl_3$	52	50:50	-
10	1d	100	DMSO	89	84/14	93
11	1d	100	n-C_6H_{14}	50	61:39	30
12	1d	100	water	85	69:31	83

[a] The reaction was performed with *p*-nitrobenzaldehyde (0.25 mmol), cyclohexanone (1.0 mmol), catalyst 1c and 1d (100 mg, 0.125 mmol g^{-1}), in the solvent (1.0 mL) at room temperature.

[b] Isolated yield after chromatography on silica gel.

[c] Determined by chiral **^{1}HNMR** analysis, major product is *anti*.

[d] Determined by chiral **HPLC** analysis of the *anti*-product.

Table 4. Effects of catalyst loading on the direct aldol reaction.[a]

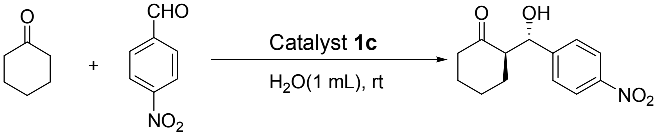

Entry	Catalyst	Cat loading[mg]	Solvents	Yield[b] (%)	anti:syn[c]	ee[d] (%)
1	1c	100	H_2O (1mL)	99	85:15	93
2	1c	80	H_2O (1mL)	99	80:20	92
3	1c	50	H_2O (1mL)	99	78:22	93
4	1c	40	H_2O (1mL)	98	84:16	92
5	1c	30	H_2O (1mL)	98	90:10	94
6	1c	20	H_2O (1mL)	98	94:6	96
7	1c	10	H_2O (1mL)	98	98:2	99
8	1c	5	H_2O (1mL)	90	98:2	95

[a] The reaction was performed with *p*-nitrobenzaldehyde (0.25 mmol), cyclohexanone (1.0 mmol), catalyst **1c**(5mg～100 mg, 0.125 mmol g^{-1}), in the presence of water (1.0 mL) at room temperature.

[b] Isolated yield after chromatography on silica gel.

[c] Determined by chiral **^{1}HNMR** analysis, major product is *anti*.

[d] Determined by chiral **HPLC** analysis of the *anti*-product.

Then, we investigated the effects of different amounts of catalyst **1c** on the reaction of cyclohexanone with *p*-nitrobenzaldehyde (**Table 4**). By using 10 mg of catalyst **1c** (0.5 mol%, 0.125 mmol/g), we obtained a good yield with excellent stereoselectivity (**Table 4**, entry 7). Therefore, the optimized amount of catalyst **1c** loading was chosen to be 10 mg (0.5 mol%, 0.125 mmol/g).

Table 5. Effects of the amount of water on the direct aldol reaction.[a]

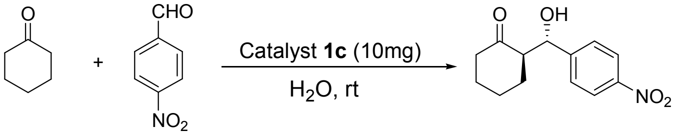

Entry	Catalyst	Cat. loading [%]	Water (mL)	Yield[b] (%)	anti:syn[c]	ee[d] (%)
1	1c	10	0.2	94	91:9	94
2	1c	10	0.4	92	89:11	94
3	1c	10	0.5	93	91:9	94
4	1c	10	0.8	91	90:10	94
5	1c	10	1.0	98	98:2	99
6	1c	10	1.5	85	91:9	92

[a] The reaction was performed with *p*-nitrobenzaldehyde (0.25 mmol), cyclohexanone (1.0 mmol), catalyst **1c** (10 mg, 0.125 mmol g^{-1}), in the presence of water at room temperature.

[b] Isolated yield after chromatography on silica gel.

[c] Determined by chiral **^{1}HNMR** analysis, major product is *anti*.

[d] Determined by chiral **HPLC** analysis of the *anti*-product.

Different results were observed with different amounts of water (**Table 5**), and the optimized amount of water was 1.0 mL. Finally, 10 mg of catalyst **1c** employed in the presence of water (1.0 mL) was the optimized catalytic condition for the direct aldol reaction between cyclohexanone and *p*-nitrobenzaldehyde.

To widen the range of substrates, we investigated ketone as an aldol donor with a series of aldehydes using catalyst **1c** in the presence of water at room temperature under the optimized reaction conditions. As revealed in **Table 6**, the processes proceeded smoothly with 10 mg (0.5 mol%, 0.125 mmol/g) of catalyst **1c** resulting in highly enantio-enriched adducts in good yields regardless of the electronic nature of the aromatic aldehydes. For the neutral and electron-rich aromatic aldehydes, a longer reaction time was required compared to that required for the electron-deficient aromatic aldehydes. However, the aldol process proceeded efficiently in good yield (99 %) with high enantioselectivity (99 %). The good performance of heterogeneous catalyst **1c** with regard to the ee value was most likely due to its novel support and good hybridization properties of the inorganic and organic components. The microenvironment of **ZrPS-PVPA-Pr** for asymmetric aldol reactions consisted of hydrophobic polystyrene potions and hydrophilic hybrid zirconium phosphonate portions with a self-assembled layered structure on the nanometre scale. Due to the interaction of a large number of polystyrene segments and layered zirconium phosphonate-phosphate existing in **ZrPS-PVPA-Pr**, a substantial number of caves, holes, pores and channels were formed due to folding, curlling, parallelling, crossing, and even twining, which resulted in the excellent catalytic performance of **1c**. However, this result is combined with the threshold effect assigned to the secondary channels, which have various sizes and shapes that are formed during the reaction in the presence of water.

Table 6. Asymmetric aldol reactions of cyclohexanone with various aromatic aldehydes in the presence of water.[a]

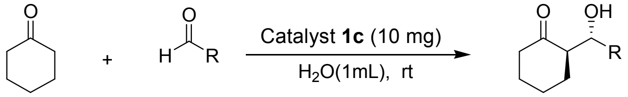

Entry	Product	Time (h)	Yield[b] (%)	anti:syn[c]	ee[d] (%)
1	2(R=*p*-NO_2-C_6H_4)	24	98	98:2	99
2	3(R=*o*-NO_2-C_6H_4)	24	99	99:1	99
3	4(R=*m*-NO_2-C_6H_4)	24	97	97:3	99
4	5(R=*p*-CN-C_6H_4)	24	98	98:2	98
5	6(R=*p*-CF_3-C_6H_4)	24	98	98:2	97
6	7(R=*p*-Br-C_6H_4)	36	95	97:3	98
7	8(R=*p*-Cl-C_6H_4)	36	96	98:2	99
8	9(R=*o*-Cl-C_6H_4)	36	95	96:4	99
9	10(R=*m*-Cl-C_6H_4)	36	92	94:6	98
10	11(R=*p*-F-C_6H_4)	36	95	96:4	98
11	13(R=*p*-OMe-C_6H_4)	36	84	93:7	96
12	14(R=*m*-OMe-C_6H_4)	36	85	94:6	97
13	15(R=2-naphthyl)	36	86	94:6	94
14	16(R=1-naphthyl)	36	87	95:5	97
15	17(R=C_6H_5)	36	85	92:8	93

[a] The reaction was performed with *p*-nitrobenzaldehyde (0.25 mmol), cyclohexanone (1.0 mmol), catalyst **1c** (10 mg, 0.125 mmol g^{-1}), in the presence of water (1.0 mL) at room temperature.

[b] Isolated yield after chromatography on silica gel.

[c] Determined by chiral ^{1}**HNMR** analysis, major product is *anti*.

[d] Determined by chiral **HPLC** analysis of the *anti*-product.

To verify that catalyst **1c** can be recovered and reused, we performed a recycling study of **1c** using the aldol reaction between cyclohexanone and *p*-nitrobenzaldehyde (**Table 7**). Catalyst **1c** was recovered by simple filtration, washed thoroughly with ethanol or water and dried at 60□ to remove all of the impurities followed by direct use in a subsequent aldol reaction without the addition of any new catalyst. In each reuse cycle, the same amount of substrate was used, and without further purification, the recovered catalyst **1c** retained its catalytic activity. In addition, only a slight decrease in the enantioselectivity was observed after **6** cycles (we did not continue beyond six cycles). In general, the layered zirconium phosphonate was relatively stable. However, the layered structure could be destroyed under some extreme conditions, such as basic solutions. However, the virgin layered structure, channels, holes and caves were roughly recovered in standing under aqueous phase conditions, which was helpful for self-assembling of the layered zirconium phosphonate. Therefore, these types of heterogeneous catalysts have the singular advantage of recyclability. The slight decrease in the activity for more cycles may be due to a physical loss during the recovery process and/or by a gradual degradation of the catalysts under the aqueous phase conditions and continuous stirring.

Table 7. Recycling and reuse of catalyst 1c[a].

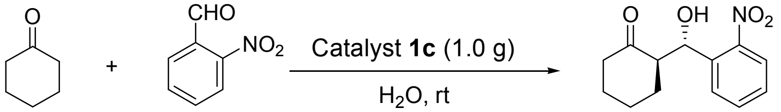

Entry	Time (h)	Yield[b] (%)	anti/syn[c]	ee[d] (%)
1	24	99	99:1	99
2	24	99	98:2	99
3	24	99	98:1	99
4	24	99	97:3	98
5	24	98	97:3	98
6	24	97	97:3	98

[a] Reaction conditions: cyclohexanone (100 mmol), aldehyde (25 mmol), catalyst **1c** (1.0 g), water (100 mL) at room temperature.

[b] The combined isolated yield of the diastereomers.

[c] Determined by chiral ^{1}**H NMR** analysis, major product is *anti*.

[d] Determined by **HPLC** analysis of the *anti* product.

In addition, the large-scale test was performed with 1 mol of an aromatic aldehyde and 4 equivalents of cyclohexanone with, the same catalyst loading (10 g, 0.5 mol%) as in the experimental scale. The experiments were facilely carried out using the same procedure as that used for the experimental scale reactions. Based on the results summarized in **Table 8**, the enantioselectivities maintained the same level in the large-scale reactions.

Table 8. Large-scale asymmetric aldol reactions.[a]

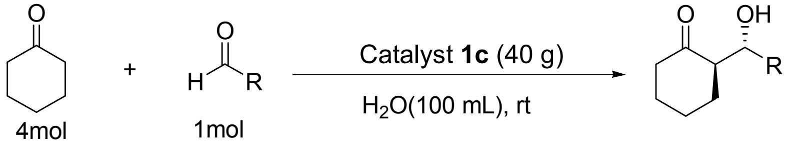

Entry	Product	Time (h)	Yield[b] (%)	anti/syn[c]	ee[d] (%)
1	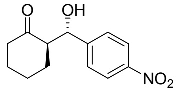	24	99	99:1	99
2	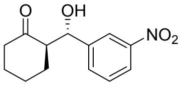	24	99	97:3	99
3	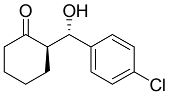	36	98	98:2	99
4	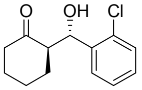	36	95	96:4	99
5	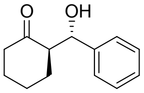	36	85	93:7	94

[a] Reaction conditions: cyclohexanone (4000 mmol), aldehyde (1000 mmol), catalyst **1c** (40 g), H_2O (4000 mL) at room temperature.

[b] The combined isolated yield of the diastereomers.

[c] Determined by chiral **HPLC** analysis, major product is *anti*.

[d] Determined by **HPLC** analysis of the *anti* product.

According to the above results (**Table 3**) where catalyst **1c** exhibited better performance in the presence of water compared to that in organic solvents, the influence of the microenvironment effect of **ZrPS-PVPA** immobilized chiral molecule with an improved hydrophilic property was due to the large number of hydroxyl groups. The exciting phenomenon was also confirmed by the layered porous micro-structure shown in **Figure 2**, which demonstrated that the organic groups in zirconium phosphonates were located on the surface of the layers, the interlamellar region and interlayer surface.

Both zirconium phosphates and zirconium phosphonates have excellent supermolecular intercalation performance. Some guests, such as amine and alkyl ethanol, can be easily intercalated into layered zirconium phosphate or zirconium phosphate-phosphonate in a polar solvent (e.g., water, ethanol or water/ethanol). According to the principle of intercalation chemistry, the interlayer distance of the zirconium phosphate or zirconium phosphate-phosphonate increased, and the layer floors were broadened in the polar solvent (i.e., water). Therefore, the heterogeneous catalyst with the layer floors of zirconium phosphates that can be distended in **ZrPS-PVPA** possess the same properties in the presence of water and can provide sufficient interspace for substrates to access to the catalytic active sites.

Conclusion

In this paper, a novel chiral phenoxy-modified organic-inorganic hybrid support-zirconium poly(styrene-phenylvinyl-phosphonate)-phosphate has been used as a catalyst support for aldol reactions, and the results highlight the versatility of this class of organic-inorganic hybrid catalyst supports. In addition, the important effects of water as a solvent for the asymmetric aldol reactions using chiral heterogeneous catalysts **1c** and **1d** have been investigated and discussed. Enantiomeric excess up to 99% was obtained along with little loss of activity and enantioselectivity, and catalyst **1c** can be efficiently used on a large-scale with the enantioselectivities of the *anti*-aldol reactions being maintained at the same level, which offers great potential for application in industry. It is easy to foresee important developments of similar systems based on insoluble **ZrPS-PVPA**. Our results also generate a new opportunity for understanding and designing organo-inorganic hybrid catalysts for chiral synthesis.

Acknowledgements

The authors are grateful to National Natural Science Foundation of China (Grant No. 41203047) and Chongqing Unis Chemical Co, Ltd of China for financial support.

Supporting Information Available

General experimental methods and spectra of the corresponding compounds are available via the Internet.

References

1 B. M. Trost, *Science*. 1991, **254**, 1471-1477.

2 A. Corma, *Chem. Rev*., 1995, **95**, 559-614.

3 W. F. Hoelderich, *Catal. Today*. 2000, **62**, 115-130.

4 E. M. Carreira, In: E. N. Jacobsen, A. Pfaltz, H. Yamamoto, *Comprehensive Asymmetric Catalysis*, 1999, 997-1065.

5 J. G. Hernández, E. Juaristi, *J. Org. Chem.,* 2011, 76, 1464-1467.

6 U. Eder, G. Sauer and R. Wiechert, *Angew. Chem, Int. Ed.,* 1971, **10**, 496-497.

7 Z. G. Hajos and D. R. Parrish, *J. Org. Chem*., 1974, **39**, 1615-1621.

8 B. List, R. A. Lerner and C. F. Barbas III., *J. Am. Chem. Soc*., 2000, **122**, 2395-2396.

9 A. Cordova, W. Notz and C. F. Barbas III., *Chem. Commun*., 2002, 3024-3025.

10 S. Bahmanyar, K. N. Houk, H. J. Martin and B. List, *J. Am. Chem. Soc*., 2003, **125**, 2475-2479.

11 A. B. Northrup, I. K. Mangion, F. Hettche and D. W. C. MacMillan, *Angew. Chem., Int. Ed*., 2004, **43**, 2152-2154.

12 Z. Tang, F. Jiang, X. Cui, L. Z. Gong, A. Q. Mi, Y.Z. Jiang and Y. D. Wu, *Proc. Natl. Acad. Sci.* U. S. A. 2004, **101**, 5755-5760.

13 D. Ender and C. Grondal, *Angew. Chem., Int. Ed*., 2005, **44**, 2.

14 U. Kazmaier, *Angew. Chem., Int. Ed*., 2005, **44**, 2186-2188.

15 L. He, Z. Tang, L. F. Cun, A. Q. Mi, Y. Z. Jiang and L. Z. Gong, *Tetrahedron.* 2006, **62**, 346-351.

16 X. Y. Xu, Z. Tang, Y. Z, Wang, S. W. Luo, L. F. Cun and L. Z. Gong, *J. Org. Chem*., 2007, **72**, 9905-9913.

17 A. Russo, G. Botta and A. Lattanzi, *Tetrahedron*. 2007, **63**, 11886-11892.

18 L. S. Zu, H. X. Xie, H. Li, J. Wang and W. Wang, *Org. Lett*., 2008, **10**, 1211-1214.

19 Y. B. Liu, Q. Tong, L. Y. Ge, Y. Zhang, L. Hua, Y. N. Fan, *RSC Adv.*, 2014, 4, 50412-50416.

20 S. P. Zhang, X. K. Fu, S. D. Fu and J. F. Pan, *Catal. Commun*., 2009, **10**, 401-405.

21 S. P. Zhang, X. K. Fu and S. D. Fu, *Tetrahedron Lett*., 2009, **50**, 1173-1176.

22 R. T. Baker and W. Tumas, *Science*. 1999, **284**, 1477-1479.

23 Q. H. Xia, H. Q. Ge, C. P. Ye, Z. M. Liu and K. X. Su, *Chem. Rev.,* 2005, **105**, 1603-1662.

24 U. Costantino, F. Fringuelli, M. Nocchetti and O. Piermatti, *Appl. Catal. A* 2007, **326**, 100-105.

25 S. J. Bae, S. W. Kim, T. Hyeon and B. M. Kim, *Chem. Commun.,* 2000, 31-32.

26 H. M. L. Davies, C. Venkataramani, T. Hansen and D. W. Hopper, *J. Am. Chem.Soc*., 2003, **125**, 6462-6463.

27 B. M. Choudary, B. K. Avita, C. N. Sreenivasa, B. Sreedhar and K. M. Lakshmi, *Catal. Lett*., 2002, **78**, 373-385.

28 M. Benaglia, M. Cinquini, F. Cozzi, A. Puglisi and G. Celentano, *Adv. Synth. Catal.,* 2002, **344**, 533-542.

29 Y. Y. Wu, Y. Z. Zhang, M. L. Yu, G. Zhao and S. W. Wang, *Org. Lett*., 2006, **8**, 4417-4420.

30 T. M. Suzuki, S. Kobayashi, D. A. Pacheco Tanaka, M. A. Llosa Tanco, T. Nagase and Y. Onodera, *React. Funct. Polym.,* 2004, **58**, 131-135.

31 A. A. Marti and J. L. Colon, *Inorg. Chem*., 2003, **42**, 2830-2832.

32 U. Costantino, M. Nocchetti and R. Vivani, *J. Am. Chem. Soc.,* 2002, **124**, 8428-8432.

33 W. S. Ren and X. K. Fu, *Catal. Commun*., 2009, **10**, 788-793.

34 I. C. Marcu, I. Sandulescu and J. M. M. Millet, *Appl. Catal.,* 2002, **227**, 309-320.

35 S. Calogero, D. Lanari, M. Orru, O. Piermatti, F. Pizzo, L. Vaccaro, *J. Catal*., 2011, 282, 112-119.

36 M. Angeloni, O. Piermatti, F. Pizzo, L. Vaccaro, *Eur. J. Org. Chem.*, 2014, 1716-1726.

37 X. J. Wu, X. B. Ma, Y. L. Ji, Q. Wang, X. Jia and X. K. Fu, *J. Mol. Catal. A*: Chem., 2007, **265**, 316-322.

38 P. A. Grieco, Organic Synthesis in Water; Ed.; Blackie Academic & Profesional: London, 1998.

39 J. M. Huang, X. T. Zhang and D. W. Armstrong, *Angew. Chem. Int. Ed.,* 2007, **46**, 9073-9077.

40 J. G. Hernández, E. Juaristi, *Chem. Commun.*, 2012, 48, 5396-5409.

41 C. L. Wu, X. K. Fu, X. B. Ma and S. Li, *Tetrahedron: Asymmetry*. 2010, **21**, 2465-2470.

42 C. L. Wu, X. K. Fu and S. Li, *Eur. J. Org. Chem.,* 2011, **7**, 1291–1299

43 C. L. Wu, X. K. Fu and S. Li, *Tetrahedron*. 2011, **67**, 4283-4290

44 C. L. Wu, X. K. Fu and S. Li, *Tetrahedron: Asymmetry*. 2011, **22**, 1063-1073.

45 C. L. Wu, X. Q. Long, S. Li and X. K. Fu, *Tetrahedron: Asymmetry*. 2012, **23**, 315-328.

46 S. Li, C. L. Wu, X. K. Fu and Q. M, *Ind. Eng. Chem. Res*., 2011, 50, 13711–13716.

47 B. W. Gong, X. K. Fu, J. X. Chen, Y. D. Li, X. C. Zou, X. B. Tu, P. P. Ding and L. P. Ma, *J. Catal*., 2009, **262**, 9-17.

Graphical Abstract

Efficient synthesis of zirconium poly(styrene-phenylvinylphos-phonate)phosphate-supported proline as a recyclable catalyst for direct asymmetric aldol reactions in water

Chuanlong Wu[a*], Xiaoqing Long[a], Xiangkai Fu[b], Guangwei Wang[c*], Zakaria. A. Mirza[c]

[a] *Chongqing Unis Chemical Co, Ltd, National Enterprise Technology Center, Chongqing, 402161, PR China*
[b] *College of Chemistry and Chemical Engineering Southwest University, Chongqing, 400715, PR China*
[c] *Chongqing Institute of Green and Intelligent Technology (CIGIT), Chinese Academy of Sciences, Chongqing, 400714, PR China*
Tel: +86 2368253704; fax: +86 2368254000
E-mail: wcl110@swu.edu.cn

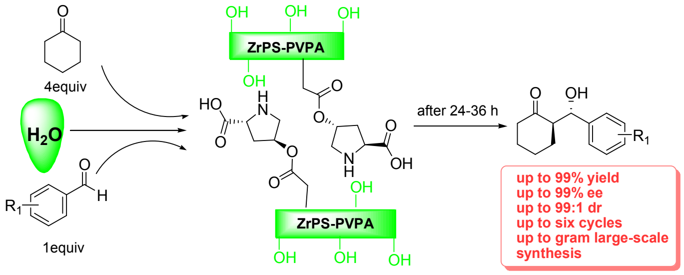

up to 99% yield
up to 99% ee
up to 99:1 dr
up to six cycles
up to gram large-scale synthesis